Polyhedral Iridamonocarbaborane Chemistry. Two Ten-vertex *arachno*-6,9-Iridacarbadecaboranes and Some Related Ten-vertex Carbaborane Chemistry. Comparative Nuclear Magnetic Resonance Studies and the Molecular Structure of [*asym*-9-(CO)-9,9-$(PPh_3)_2$-9-H-*arachno*-9,6-$IrCB_8H_{12}$] *

Xavier L. R. Fontaine, John D. Kennedy, Mark Thornton-Pett, Karl Nestor, Bohumil Štíbr, Tomáš Jelínik, and Karel Baše

School of Chemistry, University of Leeds, Leeds LS2 9JT and Institute of Inorganic Chemistry, Czechoslovak Academy of Sciences, 25068 Řež u Prahy, Czechoslovakia

Reaction of *trans*-[IrCl(CO)$(PPh_3)_2$] with [NMe_4][*nido*-6-CB_9H_{12}] in solution resulted in the formation in low yields of two isomers (*sym* and *asym*) of [9-(CO)-9,9-$(PPh_3)_2$-9-H-*arachno*-9,6-$IrCB_8H_{12}$]. These new air-stable yellow compounds differ in the arrangement of the exopolyhedral {(CO)$(PPh_3)_2$H} ligand group on the metal atom. Single-crystal *X*-ray diffraction analysis on the *asym* isomer confirmed the molecular constitution. Crystals were monoclinic, space group *Cc*, with a = 1 112.7(2), b = 2 184.7(3), c = 1 553.2(2) pm, β = 94.06(1)°, and Z = 4; 3 265 observed data [$I > 2.0\sigma(I)$]; R = 0.0183, R' = 0.0187. The cluster structure is of *arachno* ten-vertex 'boat' configuration, with the {Ir(CO)$(PPh_3)_2$} and {CH_2} centres occupying the "prow" positions 9 and 6, and with the Ir–H hydrogen atom being *endo* over the cluster open face. N.m.r. spectroscopy permits assignment of the cluster ^{11}B and ^{1}H parameters and thence comparison with the equivalent parameters of the analogues $[B_{10}H_{14}]^{2-}$, [6-CB_9H_{14}]$^-$, 6,9-$C_2B_8H_{14}$, and [5-(η^5-C_5H_5)-5,6,9-$CoC_2B_7H_{11}$], in order to assess the comparative effects of replacement of boron by carbon and metal centres in the basic ten-vertex *arachno* $[B_{10}H_{14}]^{2-}$ cluster type. Preparative details for [*arachno*-6-CB_9H_{14}]$^-$ are given.

Reported ten-vertex monoiridamonocarbaboranes are [(PPh_3)(O=CO–Me)HIrC$B_8H_7(PPh_3)$] [of schematic *closo* cluster configuration (**I**)],[1] [$(PPh_3)_2$HIrC$B_8H_8(PPh_3)$] [of schematic *closo* cluster configuration (**II**)],[2] [(PPh_3)-$(Ph_2PC_6H_4)$IrC(OH)B_8H_6(OMe)] [of schematic *isonido* cluster configuration (**III**)],[3] and a *nido* species [5-(PPh_3)-9-H-9,9-$(PPh_3)_2$-*nido*-9,6-$IrCB_8H_{10}$] [of gross configuration (**IV**)].[4] The *nido*/*arachno* ten-vertex cluster numbering scheme is as in structure (**V**). The only previously reported *arachno*-metallacarbaboranes of this configuration are the two mutually related platinum species [9,9-$(PPh_3)_2$-9,6-$PtCB_8H_{12}$][5] and [9,9-$(Ph_2PC_6H_4)_2$-9,6-$PtCB_8H_{10}$],[6] together with the ruthenium compound [9-(η^5-C_5H_5)-9-(PPh_3)-9-H-9,6-$RuCB_8H_{12}$].[7]

Here we report two new ten-vertex *arachno*-iridacarbaboranes that were isolated, as unexpected degradation products in low yield (but as the highest-yield metallacarbaborane products), from the reaction of [Ir(CO)Cl$(PPh_3)_2$] with the [*nido*-6-CB_9H_{12}]$^-$ anion. Other reported reactions of [Ir(CO)Cl$(PR_3)_2$] (R_3 = Ph_3, Me_3, Me_2Ph, *etc.*) with polyhedral boron-containing anions[8] include the reactions with [*arachno*-B_3H_8]$^-$,[9] [*arachno*-B_4H_9]$^-$,[10] [*nido*-B_5H_8]$^-$,[11] [*nido*-B_6H_9]$^-$,[12] [*nido*-B_9H_{12}]$^-$,[12] [*arachno*-B_9H_{14}]$^-$,[13–15] [*closo*-$B_{10}H_{10}$]$^{2-}$,[16,17] and [*nido*-$B_{10}H_{13}$]$^-$.[18–20] These, however, all involve binary borane anions, and, surprisingly, reactions of [Ir(CO)Cl$(PPh_3)_2$] with carbaborane anions to generate contiguous metallacarbaboranes seem to have received little, if any, attention.[21–23] By contrast, the related species [IrCl$(PPh_3)_3$] has been used in this manner with a variety of carbaborane and other heteroborane anions to generate some interesting eleven- and twelve-vertex iridacarbaborane chemistry.[2,4,24–27]

Results and Discussion

(*i*) *Reaction of* [NMe_4][CB_9H_{12}] *with* [Ir(CO)Cl$(PPh_3)_2$] *and the Isolation of* [(CO)$(PPh_3)_2$HIrCB_8H_{12}] *Isomers.*—There was no apparent initial reaction between [NMe_4]-[CB_9H_{12}] and [Ir(CO)Cl$(PPh_3)_2$] in chloroform solution, but heating under reflux for 200 h resulted in a complex mixture of products. Chromatographic separation monitored by n.m.r. spectroscopy revealed the [*closo*-1-CB_9H_{10}]$^-$ anion and triphenylphosphine–borane, $BH_3(PPh_3)$, as major products, together with a variety of coloured components present in low yield. The examination of these last by extended-accumulation Fourier-transform n.m.r. spectroscopy suggested that most consisted of polyhedral iridaboranes or carbaboranes that would repay investigation if it becomes viable to examine this reaction on a larger scale. Of these only one component was present in sufficient quantity for further reasonable investigation (yield *ca.* 8%, 300-μmol reaction scale).

The preliminary results of n.m.r. spectroscopy [subsequently extended as summarised in more detail in section (*iii*) below] suggested that this component consisted of two *arachno*-type eight-boron polyhedral iridaborane species, in an approximately 2:1 molar ratio, that were closely related. The spectra indicated that the major component had no symmetry, whereas the minor component had cluster mirror-plane symmetry. Extensive t.l.c. and h.p.l.c. work did not resolve this mixture, but attempts at fractional crystallisation ultimately gave, from chloroform–hexane, three or four small crystals, of which one

* 9-Carbonyl-9-hydrido-9,9-bis(triphenylphosphine)-6-carba-9-irida-*arachno*-decaborane.

Supplementary data available: see Instructions for Authors, *J. Chem. Soc., Dalton Trans.*, 1990, Issue 1, pp. xix—xxii.

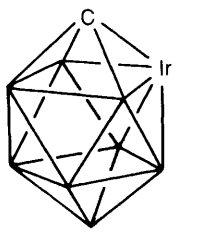

(I)

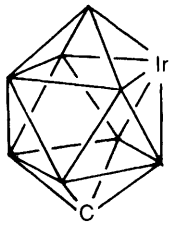

(II)

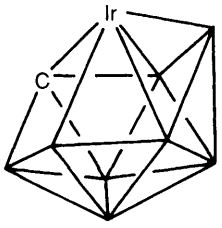

(III)

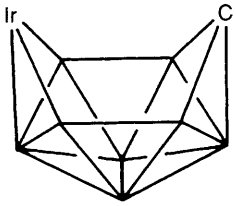

(IV)

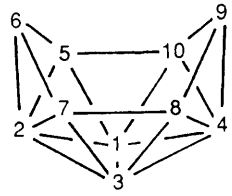

(V)

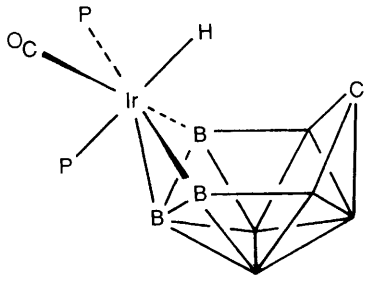

(VI)

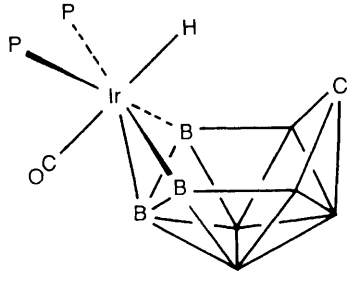

(VII)

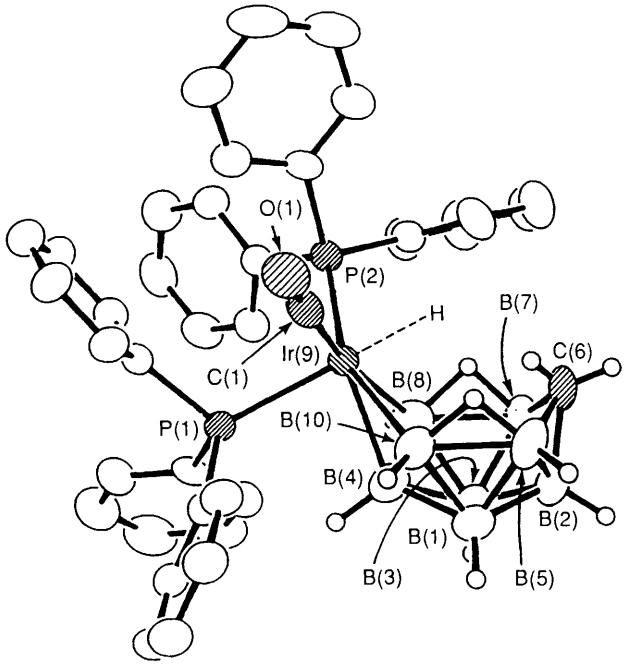

Figure 1. Drawing of the molecular structure of [*asym*-9-(CO)-9,9-$(PPh_3)_2$-9-H-*arachno*-9,6-$IrCB_8H_{12}$] (**1**). The iridium-bound hydrogen atom was not located crystallographically but is apparent from n.m.r. spectroscopy and is reasonably positioned as shown. Phenylphosphine hydrogen atoms are omitted for clarity

was found suitable for single-crystal *X*-ray diffraction analysis [see section (*ii*) below]. This work revealed that the crystals were of the asymmetric species, and identified it as [*asym*-9-(CO)-9,9-*cis*-$(PPh_3)_2$-9-*endo*-H-*arachno*-9,6-$IrCB_8H_{12}$] [compound (1), Figure 1]. Difference n.m.r. spectroscopy [section (*iii*) below] thence identified the other component as [*sym*-9-(CO)-9,9-*cis*-$(PPh_3)_2$-9-*endo*-H-*arachno*-9,6-$IrCB_8H_{12}$] (**2**), the two compounds differing only in the geometrical disposition of the $H(CO)(PPh_3)_2$ ligand group about the iridium centre [structures (**VI**) and (**VII**) respectively].

It is of interest that these ligand dispositions are the same as those reported for the two *arachno*-4-iridanonaboranes [(CO)-$(PMe_3)_2HIrB_8H_{12}$] and [$(CO)(PMe_3)_2HIrB_8H_{11}Cl$] that are obtained from the reaction of [$Ir(CO)Cl(PMe_3)_2$] with the *arachno*-$[B_9H_{14}]^-$ anion[15] in a process that involves boron-vertex loss in a $\{B_9\} \longrightarrow \{B_8\}$ degradation. The mechanism of formation of compounds (**1**) and (**2**), also involving boron-vertex loss, but now in a $\{CB_9\} \longrightarrow \{CB_8\}$ degradation, may have some parallels, but in view of the low yield of these two metallacarbaboranes any further discussion would be speculative. An oxidative process also occurs in the system, as evidenced by the identification of the [*closo*-$CB_9H_{10}]^-$ anion as a product, but there is no evidence that this contributes to metallacarbaborane formation.

(*ii*) *Molecular Structure of* [*asym*-9-(CO)-9,9-$(PPh_3)_2$-9-H-*arachno*-9,6-$IrCB_8H_{12}$] (**1**).—As mentioned in the previous section, crystals of compound (**1**) suitable for single-crystal *X*-ray diffraction analysis were obtained by diffusion of hexane into a solution of a mixture of compounds (**1**) and (**2**) in chloroform. A drawing of the molecular structure thus obtained is in Figure 1, and listings of interatomic dimensions in Tables 1 and 2. All cluster hydrogen atoms except Ir(9)–H(9)(*endo*) were located on difference maps. However, the co-ordinates of these cluster hydrogen atoms were not refined because they tended to

Table 1. Selected interatomic distances (pm) for [*asym*-9-(CO)-9,9-$(PPh_3)_2$-9-H-*arachno*-9,6-$IrCB_8H_{12}$] (**1**) with estimated standard deviations (e.s.d.s) in parentheses

(*i*) From the iridium atom			
P(1)–Ir(9)	243.3(3)		
P(2)–Ir(9)	237.1(3)	C(1)–Ir(9)	186.3(9)
B(4)–Ir(9)	225.1(8)		
B(8)–Ir(9)	229.7(9)	B(10)–Ir(9)	232.8(8)
(*ii*) Boron–boron			
B(2)–B(1)	173.7(13)	B(3)–B(2)	171.8(13)
B(3)–B(1)	178.2(13)		
B(4)–B(1)	175.6(12)	B(4)–B(3)	180.1(11)
B(5)–B(1)	180.6(14)	B(7)–B(3)	178.4(13)
B(10)–B(1)	180.8(12)	B(8)–B(3)	184.2(12)
B(5)–B(2)	177.4(14)	B(7)–B(2)	177.2(13)
B(8)–B(4)	182.0(11)	B(10)–B(4)	179.7(12)
B(10)–B(5)	190.5(12)	B(8)–B(7)	193.0(12)
(*iii*) Boron–carbon			
C(6)–B(2)	165.6(13)		
C(6)–B(5)	170.6(14)	B(7)–C(6)	175.8(13)
(*iv*) Others			
O(1)–C(1)	117.0(9)		
C(111)–P(1)	184.8(5)	C(211)–P(2)	183.9(5)
C(121)–P(1)	184.9(5)	C(221)–P(2)	182.3(5)
C(131)–P(1)	183.4(5)	C(231)–P(2)	183.8(5)

Table 2. Selected angles (°) between interatomic vectors for compound (**1**) with e.s.d.s in parentheses

(*i*) At iridium			
P(2)–Ir(9)–P(1)	103.1(2)	C(1)–Ir(9)–P(1)	88.6(3)
B(8)–Ir(9)–P(1)	103.0(3)	B(10)–Ir(9)–P(1)	101.4(3)
B(4)–Ir(9)–P(1)	82.1(3)		
C(1)–Ir(9)–P(2)	95.2(3)		
B(4)–Ir(9)–P(2)	135.4(2)	B(4)–Ir(9)–C(1)	129.3(3)
B(8)–Ir(9)–P(2)	89.3(3)	B(10)–Ir(9)–C(1)	88.1(4)
B(10)–Ir(9)–P(2)	155.3(2)	B(8)–Ir(9)–C(1)	166.3(3)
B(8)–Ir(9)–B(4)	47.1(2)	B(10)–Ir(9)–B(4)	46.2(3)
B(10)–Ir(9)–B(8)	82.4(4)		
(*ii*) About the cage open face			
B(7)–C(6)–B(5)	112.3(6)		
B(10)–B(5)–C(6)	115.1(6)	B(8)–B(7)–C(6)	114.2(6)
B(7)–B(8)–Ir(9)	118.4(5)	B(5)–B(10)–Ir(9)	118.5(6)
(*iii*) Others			
O(1)–C(1)–Ir(9)	174.0(5)		

shift by large amounts to unreasonable positions. The Ir(6)–H(6) terminal hydrogen atom was apparent from n.m.r. spectroscopy (Table 3 below), and is reasonably positioned in the *endo* position as indicated in Figure 1 and in Structure (**VI**) above (compare ref. 15).

The carbaborane fragment has clear *arachno* character, with an *endo*-terminal hydrogen atom on the C(6) position, and bridging hydrogen atoms at the B(5)B(10) and B(7)B(8) positions, as found in the *arachno* ten-vertex binary borane $[B_{10}H_{14}]^{2-}$ anion[28] and in the platinum analogue $[(PPh_3)_2$-$PtCB_8H_{12}]$[5] and also as found in related *arachno* nine-vertex species, such as 4-$(MeCN)B_9H_{13}$[29] and [4-(η^5-C_5Me_5)-4-(MeNC)-4-IrB_8H_{12}].[30] The interatomic distances within this carbaborane fragment are within normal polyhedral carbaborane ranges. The disposition of the ligands in the exopolyhedral $(CO)(PPh_3)_2H$ ligation sphere about the iridium atom is approximately orthogonal, the general orientation reasonably suggesting a basic 'octahedral' iridium(III) coordination configuration with two valencies being directed towards multicentre bonding with the open triangular B(4)B(8)B(10) unit of the carbaborane fragment as extensively discussed elsewhere[15,31,32] for related *arachno*-type species. In these terms the compound is seen to be a basic [*arachno*-$B_{10}H_{14}]^{2-}$ or $C_2B_8H_{14}$ cluster analogue in which the formal $\{BH_2\}^-$ or $\{CH_2\}$ unit in the 6 or 9 prow position is replaced by isoelectronic and isolobal $\{Ir(CO)H(PPh_3)_2\}$ which also contributes two electrons and two orbitals to the cluster bonding proper. The *arachno* ten-vertex cluster description is also in accord with Wade's electron-counting formalism if the Ir(9)–H(9) *endo*-terminal electron pair is included in the formal electron count in the same manner as *endo*-BH or *endo*-CH in a $\{BH_2\}^-$ or a $\{CH_2\}$ unit, even though it does not actually partake in the cluster bonding proper. (For a recent discussion on the effects of the incorporation of transition-element centres that contribute only two orbitals to the cluster see ref. 33.) Compound (**1**) is therefore formulated as [*asym*-9-(CO)-9,9-$(PPh_3)_2$-9-H-*arachno*-9,6-$IrCB_8H_{12}$].

(*iii*) *N.M.R. Spectroscopy.*—The ^{11}B n.m.r. spectrum of the two-component mixture of compounds (**1**) and (**2**) corresponded to that of a mixture of two *arachno*-type eight-boron species, one with some mirror-plane symmetry to generate a 1:1:2:2:2 relative intensity pattern, and the other asymmetric. The ^1H and ^{31}P n.m.r. properties of the mixture were consistent with asymmetric and symmetric exopolyhedral ligand distributions on the metal centre, for compounds (**1**) and (**2**) respectively, as depicted in structures (**VI**) and (**VII**). Integration showed that the mole ratio of asymmetric:symmetric species was *ca.* 65:35.

Because of the large molecular size and consequent short ^{11}B relaxation times,[34,35] the ^{11}B n.m.r. lines were too broad to permit successful [^{11}B–^{11}B]-correlation spectroscopy (COSY) experiments, but ^1H-{^{11}B(selective)} experiments permitted the identification of the approximate ^{11}B positions for each component, and gave their corresponding ^1H resonance positions. The (long-term accumulation) ^{11}B n.m.r. spectrum of the crystalline sample of compound (**1**) used for the single-crystal *X*-ray diffraction analysis (4×10^5 transients, 90° pulse, achieved signal-to-noise ratio = 4.9 : 1) thence permitted the confirmation of the ^{11}B and ^1H resonance lines that correspond to this asymmetric species [structure (**VI**) and Figure 1]. Difference spectroscopy thence confirmed the lines arising from the symmetric species (**2**) [of schematic structure (**VII**)]. There was no evidence for isomerisation between (**1**) and (**2**) in solution. For each compound the positions were assigned within the structures on the basis of overall ten-vertex *arachno*-type behaviour (see also Figures 2 and 3 below), together with selective sharpening of bridging ^1H resonances in ^1H-{^{11}B(selective)} experiments, and the assignments within and between the two species were all generally confirmed by the results of [^1H–^1H]-COSY-{^{11}B} spectroscopy on the mixture. The results are presented in Table 3, the only uncertainty then being among the precise assignments in compound (**1**) of the cluster positions 5, 7, 8, and 10, and of the positions 1 and 3 to one side or the other, *i.e.* as cisoid or transoid to the Ir(6)–(CO) linkage. The mass spectrum of both components gave a highest *m/z* value corresponding to the molecular ion, with principal fragments at *m/z* values corresponding to $[M - (CO)]^+$, $[M - (CO + Ph)]^+$, $[M - (CO + PPh_3)]^+$, PPh_3^+, and

Table 3. Measured n.m.r. parameters for *asym*- and *sym*-[9-(CO)-9,9-$(PPh_3)_2$-9-H-*arachno*-9,6-$IrCB_8H_{12}$] (**1**) and (**2**) respectively in $CDCl_3$ solution at 294—297 K

	Compound (**1**)[a]			Compound (**2**)[b]		
Assignment[c]	$\delta(^{11}B)$	$\delta(^1H)$[d]	Observed [^1H–^1H]-COSY correlations[e]	$\delta(^{11}B)$	$\delta(^1H)$[d]	Observed [^1H–^1H]-COSY correlations[e]
(4)	*ca.* +16	+5.05[f]	(1)vw?	*ca.* +16	+5.43	(1,3)w
(2)	*ca.* +12	+4.20	(6x)w? (6n)s (1)w? (3)w?	*ca.* +13	+4.23	(5,7)vw? (1,3)w? (6x)w? (6n)s
(5) [or (10)]	*ca.* −13	+2.56	(1)w μ(5,10)s	*ca.* −15	+1.73	(1,3)w? (μ)s
(7) [or (8)]	*ca.* −13	+1.85	(3)m μ(7,8)s			
(10) [or (5)]	*ca.* −18	+1.82	(1)w? μ(5,10)s	*ca.* −13	+2.07	(2)vw? (1,3)w (6x)w (μ)s
(8) [or (7)]	*ca.* −18	+2.58	(3)m μ(7,8)s (6x)s			
(1)	*ca.* −33	+1.34	(4)vw? (2)w? 5(w) (10)w? (3)? μ(7,8)w? μ(5,10)w?	*ca.* −31	+1.21	(4)w (2)w? (8,10)s
(3)	*ca.* −34	+0.95	(2)w? (7)m (8)m (1)? μ(7,8)w?			
μ(7,8)	—	−3.44	(7)s (8)s (3)w (6n)m	—	−3.79	(6n)m (5,7)s (8,10)s
μ(5,10)	—	−4.67	(5)s (10)s (6n)m			
(6) (*exo*)	—	+1.03	(2)w? (7)s (6n)vs	—	+1.13	(2)w? (5,7)w? (6n)s
(6) (*endo*)	—	−0.67	(2)s μ(7,8)m μ(5,10)m (6x)vs	—	−0.41	(2)s (μ)s (6x)s
(9)	—	−16.66[g]	—	—	−14.20[h]	—

[a] Additional data: $\delta(^{31}P)$ *ca.* −1.4 and *ca.* −16.2; $^2J(^{31}P–^{31}P)$ *ca.* 20 Hz. [b] Additional data: $\delta(^{31}P)$ *ca.* +5.2. [c] Assignments based on relative intensities, ^1H-{^{11}B} and {^1H–^1H}-COSY correlations, and *arachno* ten-vertex shielding patterns. [d] By ^1H-{^{11}B} spectroscopy. [e] Measured with {^{11}B} decoupling; s = strong, w = weak, m = intermediate, v = very, ? = not well defined, n = *endo*, and x = *exo*. [f] Doublet, $^3J(^{31}P–^1H)$ (cisoid) 34 Hz. [g] $^2J(^{31}P–^1H)$ (*cis*) and (*trans*), 12 and 137 Hz respectively. [h] 1:2:1 Triplet, $^3J(^{31}P–^1H)$ 18 Hz.

PPh_2^+. This overall behaviour reasonably identifies compound (**2**) as the symmetric isomer of compound (**1**).

The ^{11}B and ^1H chemical shifts for the BH(*exo*) units in compounds (**1**) and (**2**) are presented in Figure 2 (upper diagram) as a plot of $\delta(^1H)$ *versus* $\delta(^{11}B)$ for directly bound BH units. It can be seen that there is a reasonable correlation between $\delta(^1H)$ and $\delta(^{11}B)$, and there are no significant deviations, even for the positions 4, 8, and 10 adjacent to the metal position, or for the position 2 antipodal to it. This non-deviant behaviour for the 2 and 4 positions in these two *arachno* compounds is in contrast to the shielding behaviour in the *nido*-6-metalla-ten-vertex systems that have been examined, in which these two positions are often differentiated quite considerably in their ^1H shielding behaviour *versus* the general $\delta(^1H):\delta(^{11}B)$ correlation line (see, for example, refs. 36 and 37).

The presence of the $\{Ir(CO)H(PPh_3)_2\}$ moiety also appears to have little effect on the overall ^{11}B shielding behaviour of the *arachno* ten-vertex unit. The lower diagrams in Figure 2 show stick representations of the ^{11}B spectra of compound (**2**), of the neutral carbaborane analogue *arachno*-6,9-$C_2B_9H_{14}$, and of the anionic binary borane analogue [*arachno*-$B_{10}H_{14}]^{2-}$ (numerical data in Table 4 below). It can be seen from these that the basic shielding pattern is very similar indeed for all three species, the principal effect being one only of a deshielding of 5 p.p.m. or so at the metal-adjacent and metal-antipodal sites 4 and 2 in the metallacarbaborane, illustrating well the isoelectronic and isolobal relationship between the two-orbital two-electron fragments $\{BH_2\}^-$, $\{CH_2\}$, and $\{Ir(CO)H(PPh_3)_2\}$.

It is convenient also to report in this paper complete details of the assigned ^{11}B and ^1H n.m.r. behaviour of the *arachno* ten-vertex isoelectronic series that consists of 6,9-$C_2B_8H_{14}$, [6-$CB_9H_{14}]^-$, and $[B_{10}H_{14}]^{2-}$. For the neutral dicarbaborane species, only ^{11}B n.m.r. descriptions have been reported,[38–41] and for the monocarbaborane anion, only preliminary accounts.[42] The results are summarised in Tables 4 and 5, and are presented graphically in Figure 3.

The general *exo*-proton/boron-11 correlation trend (upper

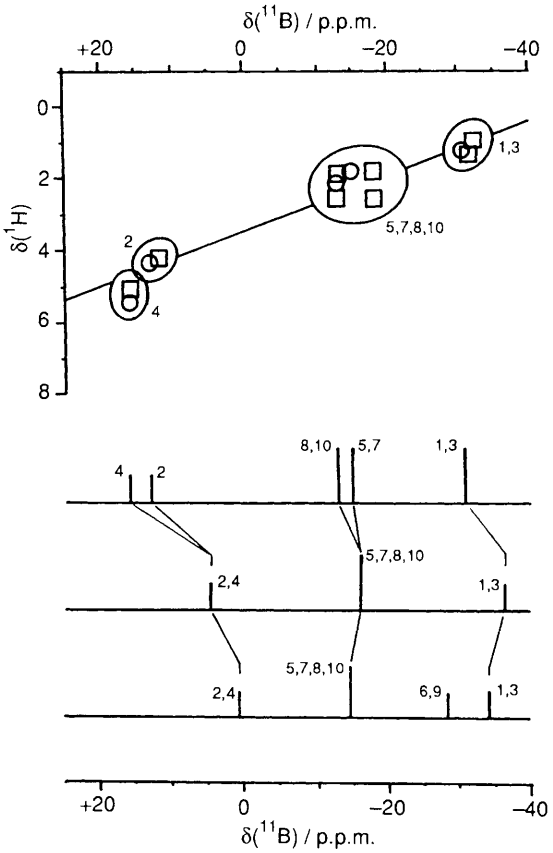

Figure 2. N.m.r. data for compounds (**1**) and (**2**) and related species. The upper diagram is a plot of $\delta(^{11}B)$ *versus* $\delta(^1H)$ for directly bound BH(*exo*) units in *sym*- and *asym*-[9-(CO)-9,9-$(PPh_3)_2$-9-H-*arachno*-9,6-$IrCB_8H_{12}$] [(**2**) (○) and (**1**) (□) respectively]. The line drawn has slope $\delta(^{11}B):\delta(^1H)$ 13:1, intercept +3.45 in $\delta(^1H)$. The lower diagram consists of stick representations of the chemical shifts and relative intensities in the ^{11}B n.m.r. spectra of compound (**2**) (top trace), *arachno*-6,9-$C_2B_8H_{14}$ (centre trace), and [*arachno*-$B_{10}H_{14}]^{2-}$ (lowest trace). Lines join equivalent positions in the three species

Table 4. Measured n.m.r. data at 294—297 K for Cs[*arachno*-6-CB_9H_{14}] (CD_3CN[a] solution), Cs_2[*arachno*-$B_{10}H_{14}$] (D_2O solution),[b] and *arachno*-6,9-$C_2B_8H_{14}$ ($CDCl_3$ solution)

	Cs[*arachno*-6-CB_9H_{14}]					Cs_2[*arachno*-$B_{10}H_{14}$]		[*arachno*-6,9-$C_2B_8H_{14}$]		
Assignment[c]	$\delta(^{11}B)$ (CD_3CN)	$\delta(^{11}B)$ (CD_2Cl_2)	$^1J(^{11}B-^1H)$	$\delta(^1H)$	Observed [$^{11}B-^{11}B$]-COSY correlations[d]	$\delta(^{11}B)$	$\delta(^1H)$	$\delta(^{11}B)$	$\delta(^1H)$	$^1J(^{11}B-^1H)$
(2)	−10.3	−9.4	150	+1.89	(1,3)s (5,7)m	+0.3	+1.96	+4.8	+2.90	162
(4)	−1.5	−1.4	138	+2.14	(1,3)w (8,10)s (9)m					
(5,7)	−13.0	−12.3	149, *ca.* 45	+2.10	(1,3)s (2)m	−15.0	+1.38	−16.4	+2.27	154,50
(8,10)	−28.8	−28.5	141, *ca.* 45	+0.64	(1,3)m (4)s (9)s					
(6)	—[e]	—	—	−0.15,[f] −1.92[g]	—	−28.6	−0.03, −1.64	—[e]	+0.86,[h] −0.68[i]	—
(9)	−23.2	−24.0	111[j]	+0.74, −0.78[k]	(4)m (8,10)s	−34.2	+0.24	−36.6	+0.93	152
(1,3)	−39.8	−39.4	139	+0.22	(2)s (4)w (5,7)s (8,10)m	—	−4.49	—	−2.85	50
μ(5,10; 7,8)	—	—	*ca.* 45[l]	−3.96[l]						

[a] Unless otherwise indicated. [b] Data from J. Rogozinski, M.Sc. Thesis, University of Leeds, 1984. [c] Assignment by relative intensities, COSY and $^1H-\{^{11}B\}$ correlations, and parallels among the three species. [d] s = Strong, w = weak, and m = intermediate. [e] Carbon atom position. [f] No significant sharpening in $^1H-\{^{11}B(5,7)$(selective)$\}$ experiment. [g] Significant sharpening in $^1H-\{^{11}B(5,7)$(selective)$\}$ experiment, implying finite $^2J(^{11}B-C-^1H)$(*endo*) of a few Hz; corresponding ^2J(*exo*) *ca.* zero (footnote *f*). [h] No significant sharpening in $^1H-\{^{11}B(5,7,8,10)$(selective)$\}$ experiment. [i] Significant sharpening in $^1H-\{^{11}B(5,7,8,10)$(selective)$\}$ experiment; see footnotes *f*—*h*. [j] Apparent 1:2:1 triplet, $^1J(^{11}B-^1H)$(mean of *exo* and *endo*) *ca.* 111 Hz (see footnote *k*). [k] Proton n.m.r. spectrum shows $^1J(^{11}B-^1H)$(*endo*) *ca.* 107 Hz (see footnote *j*). [l] Proton n.m.r. spectrum (without $\{^{11}B\}$ decoupling) shows 1:2:3:4:3:2:1 heptet pattern, mean splitting *ca.* 45 Hz.

diagram in Figure 3) is very similar to that of the isoelectronic iridacarbaboranes (**1**) and (**2**) (see Figure 2 above), with the *endo*-protons being some 1—2 p.p.m. in $\delta(^1H)$ more shielded than the general trend, and the bridging ones some 4—6 p.p.m. more shielded. These *endo* and bridging deviations are within expected ranges.[34] One interesting phenomenon is that, in contrast to the smooth transition in $\delta(^{11}B)$ for particular sites during the transition $[B_{10}H_{14}]^{2-} \longrightarrow C_2B_8H_{14} \longrightarrow [MCB_8H_{13}]$ noted above in connection with Figure 2, the ^{11}B shielding behaviour of $[CB_9H_{14}]^-$ deviates substantially from intermediacy between those of $C_2B_8H_{14}$ and $[B_{10}H_{14}]^{2-}$. In particular, although the ^{11}B nuclear shieldings of the symmetric $C_2B_8H_{14}$ and $[B_{10}H_{14}]^{2-}$ species are mutually very similar, the $^{11}B(2)$ position adjacent (*i.e.* α) to the carbon, and the $^{11}B(8,10)$ position β to the carbon, are more shielded by some 10—15 p.p.m. in the less-symmetric $[CB_9H_{14}]^-$ monocarbaborane monoanion.

A second interesting n.m.r. comparison is afforded by the ten-vertex *arachno* metalladicarbaborane [5-(η^5-C_5H_5)-*arachno*-5,6,9-$CoC_2B_7H_{13}$] [schematic configuration (**VIII**)].[43] The

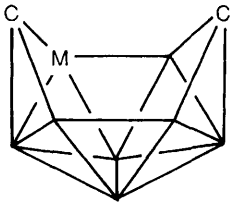

(VIII)

published n.m.r. data for this species, together with the assigned ^{11}B chemical shifts of *arachno*-6,9-$C_2B_8H_{14}$ reported here, now permit the assessment, in the *arachno* ten-vertex cluster, of the change in ^{11}B shielding effects upon the replacement of the {5-(BH)} unit by {(η^5-C_5H_5)Co} (Figure 4). When the literature assignments[43] based on [$^{11}B-^{11}B$]-COSY correlations for the cobalt compound are used (Figure 4, uppermost diagram), then there is no clear direct relationship between the two ^{11}B shielding patterns, ostensibly suggesting a severe disruption of the electronic structure of the *arachno* skeleton upon incorporation of the metal centre [contrast compound (**1**),

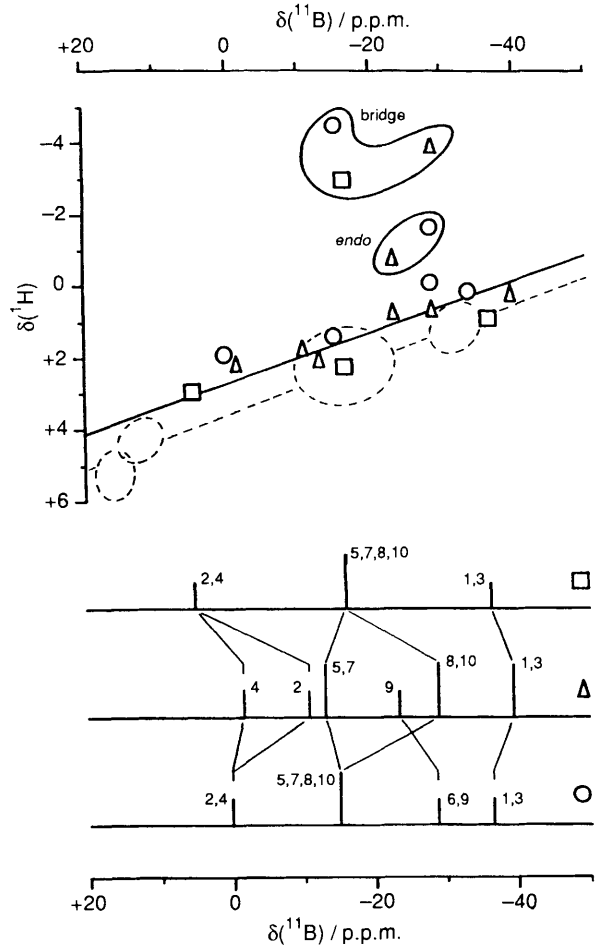

Figure 3. N.m.r. data for [*arachno*-$B_{10}H_{14}]^{2-}$ (○), [*arachno*-6-$CB_9H_{14}]^-$ (△), and *arachno*-6,9-$C_2B_8H_{14}$ (□). The upper diagram is a plot of $\delta(^{11}B)$ *versus* $\delta(^1H)$ for directly linked atoms. The solid line has slope $\delta(^{11}B):\delta(^1H)$ 14:1, intercept +2.75 in $\delta(^1H)$. The dotted lines represent the slope and cartouches from Figure 2. The lower diagram consists of stick representations of the chemical shifts and relative intensities in the ^{11}B spectra, with lines joining equivalent positions in the three species

Table 5. Non-hydrogen atom co-ordinates ($\times 10^4$) for compound (**1**) with e.s.d.s in parentheses

Atom	*x*	*y*	*z*	Atom	*x*	*y*	*z*
Ir(9)	0*	2 024.9(1)	0*	C(215)	3 632(2)	566(2)	609(2)
P(1)	−726(1)	1 453(1)	−1 276(1)	C(216)	2 427(2)	748(2)	533(2)
P(2)	326(1)	1 252(1)	1 062(1)	C(221)	−437(3)	516(1)	923(3)
C(111)	335(3)	832(1)	−1 503(2)	C(222)	−1 652(3)	525(1)	632(3)
C(112)	231(3)	264(1)	−1 105(2)	C(223)	−2 279(3)	−23(1)	496(3)
C(113)	1 131(3)	−175(1)	−1 165(2)	C(224)	−1 691(3)	−581(1)	650(3)
C(114)	2 134(3)	−47(1)	−1 624(2)	C(225)	−476(3)	−589(1)	941(3)
C(115)	2 238(3)	521(1)	−2 022(2)	C(226)	151(3)	−41(1)	1 077(3)
C(116)	1 338(3)	961(1)	−1 962(2)	C(231)	−98(4)	1 481(2)	2 138(2)
C(121)	−783(3)	1 913(2)	−2 277(2)	C(232)	−951(4)	1 146(2)	2 556(2)
C(122)	193(3)	2 290(2)	−2 426(2)	C(233)	−1 269(4)	1 325(2)	3 371(2)
C(123)	207(3)	2 616(2)	−3 197(2)	C(234)	−734(4)	1 840(2)	3 768(2)
C(124)	−755(3)	2 565(2)	−3 820(2)	C(235)	119(4)	2 175(2)	3 350(2)
C(125)	−1 731(3)	2 188(2)	−3 671(2)	C(236)	437(4)	1 996(2)	2 535(2)
C(126)	−1 745(3)	1 862(2)	−2 900(2)	C(1)	1 546(6)	1 985(2)	−386(4)
C(131)	−2 185(3)	1 059(2)	−1 389(3)	O(1)	2 525(4)	2 015(2)	−612(3)
C(132)	−3 155(3)	1 279(2)	−957(3)	B(1)	−1 491(7)	3 446(3)	−360(5)
C(133)	−4 268(3)	983(2)	−1 054(3)	B(2)	−1 624(8)	3 652(4)	709(5)
C(134)	−4 411(3)	468(2)	−1 582(3)	B(3)	−2 446(7)	3 036(3)	311(5)
C(135)	−3 442(3)	249(2)	−2 014(3)	B(4)	−1 543(6)	2 644(3)	−434(4)
C(136)	−2 329(3)	544(2)	−1 918(3)	B(5)	−171(8)	3 674(3)	307(6)
C(211)	1 929(2)	1 045(2)	1 219(2)	C(6)	−419(7)	3 452(3)	1 333(5)
C(212)	2 635(2)	1 160(2)	1 979(2)	B(7)	−1 714(7)	2 994(3)	1 369(5)
C(213)	3 839(2)	979(2)	2 055(2)	B(8)	−1 746(6)	2 295(4)	609(4)
C(214)	4 338(2)	681(2)	1 370(2)	B(10)	−122(7)	3 025(3)	−509(5)

* Co-ordinate fixed to define origin.

Figure 2 above]. However, we would propose an alternative assignment for the cobalt compound (Figure 4, lowest diagram) that is also consistent with the published [^{11}B–^{11}B]-COSY work and that, we believe, is much more consistent with the cluster *arachno* character. When our assignments for the cobaltadicarbaborane are used the principal deviations from the shielding pattern of the *arachno*-6,9-$C_2B_8H_{14}$ parent are then limited to deshieldings at the ^{11}B(1) and ^{11}B(2) positions adjacent to the Co(5) site. This α-deshielding phenomenon is a feature also in *nido* ten-vertex clusters,[44] and a related α-deshielding effect also obtains in *closo* twelve-vertex clusters.[45–47]

Experimental

Preparation of [$NHMe_3$][*nido*-6-CB_9H_{12}] *and* [NMe_4][*nido*-6-CB_9H_{12}].—A modification of the literature method[48] was adopted. The aqueous solution of Na[6-CB_9H_{12}] from the reported synthesis[48] was reduced in volume to *ca.* 20 cm^3, and aqueous [$NHMe_3$]Cl solution (1 mol dm^{-3}, 20 cm^3) added. The resulting white precipitate was filtered off under suction and dried *in vacuo* at 295—300 K to give typically 2.5 g [13.75 mmol, 55% based on 6-(NMe_3)-*nido*-6-CB_9H_{11} consumed] of [$NHMe_3$][6-CB_9H_{12}]. The filtrate was treated with [NMe_4]Cl (1 mol dm^{-3}, 10 cm^{-3}), and the resulting white precipitate filtered off under suction and dried *in vacuo* at 295—300 K to give typically 1.2 g (6.25 mmol, 25%) of [NMe_4][6-CB_9H_{12}].

Preparation of Cs[*arachno*-6-CB_9H_{14}] *and* [NMe_4][*arachno*-6-CB_9H_{14}].—The procedure was as summarised in a preliminary communication.[42] Sodium metal (1.4 g, 60 mmol) was added in several portions to a stirred suspension of [$NHMe_3$][6-CB_9H_{12}] (made as above; 3.60 g, 20 mmol) in NH_3 (70 cm^3) at 195 K (solid CO_2 bath), a dry nitrogen atmosphere being maintained throughout. The resulting mixture was allowed to reflux under stirring (bath at 243 K) for 8 h, then cooled to 195 K, and treated with solid [NH_4]Cl (3.3 g, 60 mmol). The ammonia was removed by evaporation, and the solid residue dissolved in aqueous NaOH solution (5% w/v, 50 cm^3). The resulting solution was filtered in air, and aqueous CsCl solution (1 mol dm^{-3}, 20 cm^3) added. The resulting white solid was filtered off under suction, washed with cold water (273 K, *ca.* 20 cm^3), and dried *in vacuo* at 295—300 K to give typically 3.1 g (12 mmol, 60%) of Cs[6-CB_9H_{14}], identified as such by ^{1}H, ^{13}C, ^{11}B, and [^{11}B–^{11}B]-COSY n.m.r. spectroscopy (ref. 41, see also Table 4). Analytical samples may be obtained by slow evaporation of acetonitrile from a saturated solution in toluene–acetonitrile (50:50). The aqueous solution remaining after filtration of the Cs[6-CB_9H_{14}] was treated with aqueous [NMe_4]Cl solution (1 mol dm^{-3}, 10 cm^3), and the resulting white precipitate filtered off under suction and dried *in vacuo* at 295—300 K to give typically 1.2 g (6 mmol, 30%) of [NMe_4][6-CB_9H_{14}], the total yield of the [*arachno*-6-CB_9H_{14}]$^-$ anion being typically 18 mmol (90%).

Preparation of [9-(CO)-9,9-$(PPh_3)_2$-9-H-*arachno*-9,6-$IrCB_8H_{10}$] (**2**) *and* (**2**).—A suspension made from [Ir(CO)Cl(PPh_3)$_2$] (300 mg, 0.58 mmol) and [NMe_4][6-CB_9H_{12}] (made as above; 600 mg, 3.07 mmol) in dry, degassed chloroform (40 cm^3) was heated under reflux for 8 d (nitrogen atmosphere), during which time the original yellow solution/white suspension darkened to orange and buff respectively. The solution was filtered off with the aid of more chloroform (20 cm^3), the orange filtrate reduced in volume to *ca.* 10 cm^3, and then applied to a series of preparative t.l.c. plates [200 × 200 × 1 mm, made on glass formers from an aqueous slurry of silica gel G (Fluka type GF254) followed by drying in air at *ca.* 353 K]. Development with chloroform–hexane (80:20) gave a series of coloured bands which was divided into three zones: (*a*) R_f 0.99—0.41, (*b*) R_f 0.40—0.19, and (*c*) R_f 0.18—0.00. Each zone was washed from the silica using CH_2Cl_2–MeCN (80:20), and evaporated to dryness (rotary evaporator, water-pump pressure, bath at *ca.* 298 K). Sample (*a*) was subjected to separation by h.p.l.c. [silica

column (Knauer, Lichrosorb Si60 (7 μm mesh); 25 cm × 16 mm; n-C_6H_{14}–CH_2Cl_2 (10:90) as liquid phase, flow rate 6 cm^3 min^{-1}; detection by u.v. absorption at 260 nm], giving two fractions: (*i*) retention time (R_t) 12.7—18.0 min (orange) and (*ii*) R_t 18.0—20.8 min (pale yellow). Fraction (*i*) was reduced to dryness (rotary evaporator, water-pump pressure, bath at *ca.* 298 K), and further separated by h.p.l.c. [as above, but now using n-C_6H_{14}–CH_2Cl_2 (35:75) as liquid phase], the fraction with R_t 10.4—12.9 min being collected as an orange solution. This was reduced to dryness as above, taken up in the minimum of $CHCl_3$, and a layer of n-C_6H_{14} was carefully applied to the top of the $CHCl_3$ solution. Diffusion of the hexane over a few days resulted in the formation of a colourless microcrystalline solid that mass spectrometry and n.m.r. spectroscopy (see text and Table 3) showed was a mixture of [*asym*- and *sym*-9-(CO)-9,9-$(PPh_3)_2$-9-H-*arachno*-9,6-$IrCB_8H_{12}$] (**1**) and (**2**) respectively (27 mg, 31 μmol; 8.2%). Attempts at fractional crystallisation to separate these components by diffusion of hexane into solutions in CH_2Cl_2 resulted on one occasion in the formation of four small crystals. One of these was suitable for single-crystal *X*-ray diffraction analysis (see below) and was shown to be the asymmetric isomer (**1**).

Isolation of [*closo*-1-CB_9H_{10}]$^-$ *from the Reaction of* [Ir(CO)Cl$(PPh_3)_2$] *with* [NMe_4][6-CB_9H_{12}].—The t.l.c. fraction (*c*), with R_f 0.18—0.00, from the above reaction mixture was subjected to h.p.l.c. separation using CH_2Cl_2–MeCN (98:2) as liquid phase, other conditions being as specified above. The product [NMe_4][1-CB_9H_{10}] was isolated as a colourless solid (38 mg, 190 μmol; 6.3%) by removal of the volatile components (rotary evaporator, water-pump pressure, bath at *ca.* 298 K) from the colourless fraction with R_t centred on 9.7 min. The anion was identified by its n.m.r. properties as follows {ordered as assignment, δ(^{11}B) [δ(^{1}H) of directly bound H atom] (relative intensity)}: BH(10) + 28.9 [+5.44] (1 BH), BH (2,3,4,5) −19.2 [+1.50] (4 BH), BH(6,7,8,9) −24.7 [+0.70] (4 BH), and CH(1) [+4.90] (1 CH); $CDCl_3$ solution at 294 K.

N.M.R. Spectroscopy.—N.m.r. spectroscopy was performed at 2.35 and 9.4 T using commercially available instrumentation. The general techniques, and the techniques of [^{11}B–^{11}B]-COSY,[49] [^{1}H–^{1}H]-COSY-{^{11}B},[35] and ^{1}H-{^{11}B}[50] n.m.r. spectroscopy, were essentially as described and illustrated in other recent papers describing n.m.r. work in our laboratories.[45,51–54] Chemical shifts δ are given in p.p.m. positive to high frequency (lower nuclear shielding field) of Ξ 100 ($SiMe_4$) for ^{1}H (quoted ±0.05 p.p.m.), Ξ 40.480 730 (nominally 85% H_3PO_4) for ^{31}P (quoted ±0.5 p.p.m.), and Ξ 31.083 971 MHz (nominally $F_3B{\cdot}OEt_2$ in $CDCl_3$) for ^{11}B (quoted ±0.5 p.p.m.), Ξ being defined as in ref. 55. Coupling constants $^1J(^{11}B–^{11}B)$ are given in Hz, and were measured from resolution-enhanced ^{11}B spectra with digital resolution 8 Hz.

Mass Spectrometry.—This was carried out on an A.E.I. (now Kratos) MS30 instrument using 70 eV (1.12×10^{-17} J) electron-impact ionisation and a standard solid-sample introduction probe. Calibration was by perfluorokerosene (pfk).

Single-crystal X-Ray Diffraction Analysis of Compound (**1**).—All crystallographic measurements were made on a Nicolet P3/F diffractometer operating in the ω—2θ scan mode, essentially following a standard crystallographic procedure described in detail elsewhere.[56] The data set was corrected for absorption empirically once the structure had been determined.[57]

The structure was determined *via* standard heavy-atom methods and refined by a full-matrix least squares using the SHELX program system.[58] All non-hydrogen atoms were refined with anisotropic thermal parameters. The phenyl groups were treated as rigid bodies and were refined with idealised hexagonal symmetry. The phenyl hydrogen atoms were included in calculated positions and assigned to an overall isotropic parameter. The carbaborane cluster hydrogen atoms were located on a Fourier difference synthesis. However, they proved unstable to free refinement and were therefore assigned a fixed isotropic thermal parameter and were fixed in their found positions. The weighting scheme $w = [\sigma^2(F_o) + g(F_o)^2]^{-1}$ was used at the end of refinement in order to obtain a flat analysis of variance for increasing sin θ and $(F/F_{max.})^{\frac{1}{2}}$. Final non-hydrogen atomic co-ordinates are given in Table 5.

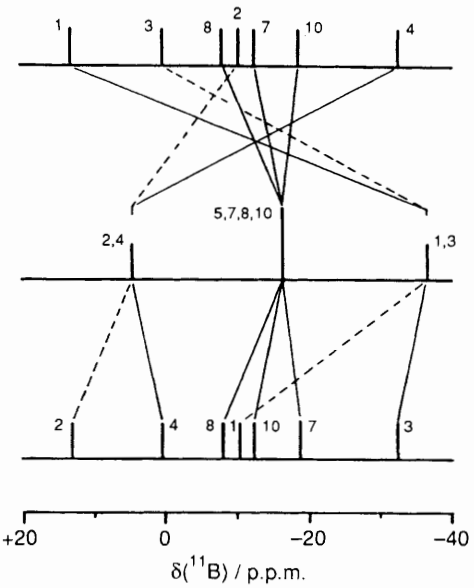

Figure 4. Stick diagrams representing the ^{11}B chemical shifts in n.m.r. spectra of the species *arachno*-6,9-$C_2B_8H_{14}$ (centre trace) and [5-(η^5-C_5H_5)-*arachno*-5,6,9-$CoC_2B_7H_{13}$] (uppermost and lowest traces). In the uppermost diagram the assignments of ref. 43 are used, whereas the lower diagram uses our suggested assignments (see text). Lines join equivalent positions in the two species, with the dotted line signifying positions adjacent (α) to the meal atom

Crystal data. $C_{38}H_{43}B_8IrOP_2$, M = 856.41, monoclinic, space group *Cc*, a = 1 112.7(2), b = 2 184.7(3), c = 1 553.2(2) pm, β = 94.06(1)°, U = 3.766 3(9) nm^3, Z = 4, D_c = 1.51 Mg m^{-3}, μ = 35.03 cm^{-1}, $F(000)$ = 1 704.

Data collection. Scan widths 2.0° + α-doublet splitting, scans speeds 2.0—29.3° min^{-1}, 4.0 < 2θ < 50.0°. 3 508 Data collected, 3 265 with $I > 2.0\sigma(I)$ considered observed, T = 290 K.

Structure refinement. Number of parameters = 378, g = 0.0004, R = 0.0183, R' = 0.0187.

Additional material available from the Cambridge Crystallographic Data Centre comprises H-atom co-ordinates, thermal parameters, and remaining interatomic distances and angles.

Acknowledgements

We thank the British Council, the Royal Society, and Borax Research Limited for support, the S.E.R.C. for equipment grants, Dr. J. B. Farmer and Professor N. N. Greenwood for their interest, and Mr. D. Singh for mass spectrometry.

References

1 J. E. Crook, N. N. Greenwood, J. D. Kennedy, and W. S. McDonald, *J. Chem. Soc., Chem. Commun.*, 1983, 83.
2 N. W. Alcock, J. G. Taylor, and M. G. H. Wallbridge, *J. Chem. Soc., Chem. Commun.*, 1983, 1168.
3 J. E. Crook, N. N. Greenwood, J. D. Kennedy, and W. S. McDonald, *J. Chem. Soc., Chem. Commun.*, 1981, 933.

4 N. W. Alcock, J. G. Taylor, and M. G. H. Wallbridge, *Acta Crystallogr., Sect. C*, 1988, **44**, 2079.
5 G. A. Kukina, I. A. Zakharova, M. A. Porai-Koshits, B. Štíbr, P. S. Sergienko, K. Baše, and J. Dolanský, *Izv. Akad. Nauk SSSR, Ser. Khim.*, 1978, **9**, 1228; G. A. Kukina, S. V. Sergienko, M. A. Porai-Koshits, K. Baše, and I. A. Zakharova, *ibid.*, 1981, **12**, 2838.
6 K. Baše, B. Štíbr, G. A. Kukina, and I. A. Zakharova, *Proc. 8th Conf. Coord. Chem., Smolenice*, 1980, pp. 17—19 (*Chem. Abstr.*, 1981, **95**, 23933g).
7 N. W. Alcock, M. J. Jasztal, and M. G. H. Wallbridge, *J. Chem. Soc., Dalton Trans.*, 1987, 2793.
8 J. D. Kennedy, *Prog. Inorg. Chem.*, 1984, **32**, 519; 1986, **34**, 211 and refs. therein.
9 J. Bould, N. N. Greenwood, J. D. Kennedy, and W. S. McDonald, *J. Chem. Soc., Dalton Trans.*, 1985, 1843.
10 S. K. Boocock, M. E. Toft, K. E. Inkrott, L-Y. Hsu, J. C. Huffman, K. Folting, and S. G. Shore, *Inorg. Chem.*, 1984, **23**, 3084.
11 N. N. Greenwood, J. D. Kennedy, W. S. McDonald, D. Reed, and J. Staves, *J. Chem. Soc., Dalton Trans.*, 1979, 117.
12 J. Bould, N. N. Greenwood, and J. D. Kennedy, *J. Chem. Soc., Dalton Trans.*, 1982, 481.
13 S. K. Boocock, J. Bould, N. N. Greenwood, J. D. Kennedy, and W. S. McDonald, *J. Chem. Soc., Dalton Trans.*, 1982, 713.
14 J. Bould, J. E. Crook, N. N. Greenwood, J. D. Kennedy, and W. S. McDonald, *J. Chem. Soc., Chem. Commun.*, 1982, 346.
15 J. Bould, J. E. Crook, N. N. Greenwood, and J. D. Kennedy, *J. Chem. Soc., Dalton Trans.*, 1984, 1903.
16 J. E. Crook, N. N. Greenwood, J. D. Kennedy, and W. S. McDonald, *J. Chem. Soc., Chem. Commun.*, 1982, 383.
17 J. E. Crook, Ph.D. Thesis, University of Leeds, 1982.
18 F. Klanberg, P. A. Wegner, G. W. Parshall, and E. L. Muetterties, *Inorg. Chem.*, 1968, **7**, 2072.
19 A. R. Siedle, *J. Organomet. Chem.*, 1975, **97**, C4.
20 A. R. Siedle and L. J. Todd, *Inorg. Chem.*, 1976, **15**, 2838.
21 R. N. Grimes, in 'Comprehensive Organometallic Chemistry,' eds. G. Wilkinson, F. G. A. Stone, and E. Abel, Pergamon, Oxford, 1982, part 1, p. 459.
22 A. J. Welch, *Annu. Rep. Chem. Soc. (London), Sect. A*, 1981–1983 and refs. therein.
23 R. Greatrex, *Annu. Rep. Chem. Soc. (London), Sect. A*, 1984–1987 and refs. therein.
24 C. W. Jung and M. G. Hawthorne, *J. Am. Chem. Soc.*, 1980, **102**, 3024 and refs. therein.
25 R. T. Baker, *Inorg. Chem.*, 1986, **25**, 109.
26 K. Nestor, X. L. R. Fontaine, N. N. Greenwood, J. D. Kennedy, J. Plešek, B. Štíbr, and M. Thornton-Pett, *Inorg. Chem.*, 1989, **28**, 2219.
27 Faridoon, O. Ni Dhubhghaill, T. R. Spalding, G. Ferguson, B. Kaitner, X. L. R. Fontaine, J. D. Kennedy, and D. Reed, *J. Chem. Soc., Dalton Trans.*, 1988, 2739.
28 D. S. Kendall and W. N. Lipscomb, *Inorg. Chem.*, 1973, **12**, 546.
29 F. E. Wang, P. G. Simpson, and W. N. Lipscomb, *J. Chem. Phys.*, 1961, **35**, 1335.
30 K. Nestor, X. L. R. Fontaine, N. N. Greenwood, J. D. Kennedy, and M. Thornton-Pett, *J. Chem. Soc., Dalton Trans.*, 1989, 1465.
31 J. Bould, N. N. Greenwood, and J. D. Kennedy, *J. Chem. Soc., Dalton Trans.*, 1984, 2477.
32 Faridoon, O. Ni Dhubhghaill, T. R. Spalding, G. Ferguson, X. L. R. Fontaine, and J. D. Kennedy, *J. Chem. Soc., Dalton Trans.*, 1989, 1657.
33 J. D. Kennedy, *Main Group Metal Chem.*, 1989, **12**, 149.
34 See, for example, J. D. Kennedy, in 'Multinuclear NMR,' ed. J. Mason, Plenum, London and New York, 1987, ch. 8, pp. 221—254, and refs. therein.
35 X. L. R. Fontaine and J. D. Kennedy, *J. Chem. Soc., Chem. Commun.*, 1986, 779.
36 N. N. Greenwood, J. D. Kennedy, I. Macpherson, and M. Thornton-Pett, *Z. Anorg. Allg. Chem.*, 1986, **54**, 45.
37 M. Bown, X. L. R. Fontaine, N. N. Greenwood, and J. D. Kennedy, *J. Organomet. Chem.*, 1987, **325**, 233.
38 B. Štíbr, J. Plešek, and S. Heřmánek, *Chem. Ind. (London)*, 1972, 649.
39 B. Štíbr, J. Plešek, and S. Heřmánek, *Collect. Czech. Chem. Commun.*, 1974, **39**, 1805.
40 Z. Janoušek, J. Plešek, S. Heřmánek, and B. Štíbr, *Polyhedron*, 1985, **4**, 1797.
41 B. Štíbr, Z. Janoušek, J. Plešek, T. Jelínek, and S. Heřmánek, *Collect. Czech. Chem. Commun.*, 1987, **52**, 103.
42 B. Štíbr, T. Jelínek, J. Plešek and S. Heřmánek, *J. Chem. Soc., Chem. Commun.*, 1987, 963.
43 J. J. Briguglio and L. G. Sneddon, *Organometallics*, 1986, **5**, 327.
44 M. Bown, X. L. R. Fontaine, H. Fowkes, N. N. Greenwood, J. D. Kennedy, P. Mackinnon, and K. Nestor, *J. Chem. Soc., Dalton Trans.*, 1988, 2597.
45 M. Bown, J. Plešek, K. Baše, B. Štíbr, X. L. R. Fontaine, N. N. Greenwood, and J. D. Kennedy, *Magn. Reson. Chem.*, 1989, **27**, 947.
46 Faridoon, M. McGrath, T. R. Spalding, X. L. R. Fontaine, J. D. Kennedy, and M. Thornton-Pett, *J. Chem. Soc., Dalton Trans.*, 1990, 1819.
47 K. Nestor, T. Jelínek, X. L. R. Fontaine, N. N. Greenwood, J. D. Kennedy, M. Thornton-Pett, S. Heřmánek, and B. Štíbr, *J. Chem. Soc., Dalton Trans.*, 1990, 681.
48 K. Baše, B. Štíbr, J. Donalský, and J. Duben, *Collect. Czech. Chem. Commun.*, 1981, **46**, 2345.
49 T. L. Venable, W. C. Hutton, and R. N. Grimes, *J. Am. Chem. Soc.*, 1984, **106**, 29.
50 J. D. Kennedy and N. N. Greenwood, *Inorg. Chim. Acta*, 1980, **38**, 529.
51 X. L. R. Fontaine and J. D. Kennedy, *J. Chem. Soc., Dalton Trans.*, 1987, 1573.
52 M. A. Beckett, M. Bown, X. L. R. Fontaine, N. N. Greenwood, J. D. Kennedy, and M. Thornton-Pett, *J. Chem. Soc., Dalton Trans.*, 1988, 1969.
53 M. Bown, X. L. R. Fontaine, and J. D. Kennedy, *J. Chem. Soc., Dalton Trans.*, 1988, 1467.
54 G. Ferguson, J. D. Kennedy, X. L. R. Fontaine, Faridoon, and T. R. Spalding, *J. Chem. Soc., Dalton Trans.*, 1988, 2555.
55 W. McFarlane, *Proc. R. Soc. London, Ser. A*, 1965, **306**, 185.
56 A. Modinos and P. Woodward, *J. Chem. Soc., Dalton Trans.*, 1974, 2065.
57 N. Walker and D. Stuart, *Acta Crystallogr., Sect. A*, 1983, **39**, 158.
58 G. M. Sheldrick, SHELX 76, Program System for *X*-Ray Structure Determination, University of Cambridge, 1976.

Received 24*th January* 1990; *Paper* 0/00391C